

SELECTIVE POSITION SENSITIVE PHOTORECEIVERS

V. Dorogan, T. Vieru

Technical University of Moldova

INTRODUCTION

Photoreceivers with one- or two-coordinate (photodiode-quadrant) sensitivity are used in optoelectronic systems for precision determining of space position of radiation source or objects reflecting radiation what is emitted from special source [1]. Optoelectronic devices made on the basis of photoreceivers with coordinate sensitivity permits to introduce automation into production process, to orientate and direct the high velocity objects in space, to realize alarm system etc. For these photoreceivers atmosphere is transmission medium of optical signals. For effective work photosensitivity spectra of these devices must coincides with the windows of "transparency" in atmosphere, where absorption losses are the minimum. This aim may be attained by creation of photoreceivers with selective photosensitivity in these spectral regions. Wavelength $\lambda = 1.06 \mu\text{m}$ corresponds to one of such windows of "transparency". Photoreceivers with maximum of photosensitivity spectra for $\lambda = 1.06 \mu\text{m}$ have very small photosensitivity to background radiation and therefore they have high trouble protection [2]. Until this problem was solved by using additional interference optic filter, what complicates essence of receiving module and decreases the conversion efficiency of optic signal received.

1. THE STRUCTURE OF SELECTIVE PHOTORECEIVER AND TECHNOLOGY OF ITS FORMING

To obtain maximum of photosensitivity spectra for $\lambda = 1.06 \mu\text{m}$ and to exclude influence of visible and infrared spectrum regions InP-InGaAsP heterostructure having two layers with different composition and respectively different band gap width was used. It was grown by the method of liquid phase epitaxy (LPE) from In-liquid melts. To compare with molecular beam epitaxy (MBE) and metalloorganic compound vacuum deposition (MOCVD), the method of LPE without any difficulties provides the growth of epitaxial layers of InGaAsP with thickness more that $5 \mu\text{m}$,

necessary for the achievement of good selectivity of realized photoreceivers photosensitivity [3].

Analyzing the recent investigations in this field of microelectronics, we have chosen the p-i-n structure for creation the photodiode-quadrant with selective photosensibility. The main parameters of the layers, which determine the effective function of p-i-n diode, are the concentration (n_d) and the mobility of charge carriers (electrons) in them. To obtain low dark current (I_d), high breakdown voltage of p-i-n junction, low own capacities (C_i), extension of space charge region on the whole thickness of the active layers, n_d has to be not bigger than $10^{12} - 5 \cdot 10^{15} \text{ cm}^{-3}$. Usually, the background concentration of ionized impurities in epitaxial layers of InGaAsP without any additional purified procedures is $(1-5) \cdot 10^{17} \text{ cm}^{-3}$. Our experiments have shown that a preventive $700 \text{ }^\circ\text{C}$ thermal treatment of liquid phases can promote to decrease the doped level below 10^{17} cm^{-3} . Thus we reduced the n_d value to $2 \cdot 10^{15} \text{ cm}^{-3}$. But, it was determined that the increasing of thermal treatment duration led to increase of compensation in the layers and decrease of electron mobility. The further reduce of doped level and compensation degree was possible by introducing the metal Gd, Yb, Tb, Dy, Y, Ho etc. in the liquid melt-solution. We determined that the most effective and preferable was yttrium (Y).

Summarizing the results of experiments connected with doping of epitaxial layers by Y, we have to mark the following: the doped level n_d can be reduced to the values closed the own concentration in InGaAs ($n_i \sim 10^{12} \text{ cm}^{-3}$) by increase the concentration of Y in melt-solution; an inversion of conductivity type in epitaxial layers (from n-type to p-type) occurs at certain values of X_Y ; the probability of conductivity type inversion increases with increasing of uncontrollable impurities background; as a rule, the electron mobility decreases with increases of Y quantity in melt-solution.

The analysis of the literature and our investigation results permit us to assume the next action mechanism of these metals in liquid melt-solution. Being chemical very active, these elements tie up the impurities from solution, especially elements of group VI (donors), and decreases their

segregation coefficient in the growing layer of InGaAsP. With elements of group II these metals interact weaker. It was determined, also, that used metals interact with oxygen from melt-solution and with As, forming the complexes of type Me_xAs_y , which become getter for background impurities.

The structure of selective photoreceiver is shown in Fig.1. It consists of n^+ InP substrate ($E_g = 1.35$ eV); InGaAsP epitaxial layer ($E_g = 1.12$ eV), serving as the active layer where useful signal with $\lambda = 1.06$ μm is absorbed and photogenerated charge carriers are separated; InGaAsP frontal epitaxial layer ($E_g = 1.18$ eV), serving as the optic filter.

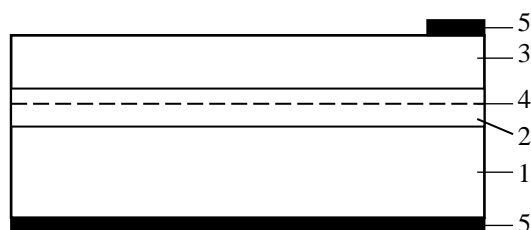


Figure 1. The structure of selective receiver. 1 – n^+ InP substrate; 2 – InGaAsP active layer ($E_g = 1.12$ eV); 3 – InGaAsP frontal layer ($E_g = 1.18$ eV); 4 – p-n junction; 5 – metal contacts.

The p-n junction was formed by planar or local low temperature Zn diffusion from Sn:Zn source. To prevent the surface erosion of epitaxial structures diffusion in quasi-closed volume with superfluous pressure of phosphorus was made. The p-n junction was placed in InGaAsP ($E_g = 1.12$ eV) active layer with thickness $3\div 5$ μm and low concentration of charge carriers ($n^0 \approx 2 \cdot 10^{15}$ cm^{-3}). The space charge region of p-n junction is localized only in active layer and doesn't extend in neighboring layers for back bias voltage.

Frontal layer of heterostructure absorbs the most part of radiation if condition $\alpha \cdot d \geq 1$ is satisfied, where α is absorption coefficient, d is frontal layer thickness. On the other hand, frontal layer thickness has to be bigger than diffusion length of minority charge carriers generated in frontal layer by high energy photons. When these conditions are realized radiation with photons energy $h\nu \geq 1.18$ eV doesn't make any contribution to photocurrent formation.

The spectral characteristics of our selective photodiode-quadrant on the basis of InP-InGaAsP heterostructure and of Si industrial photoreceiver optimized for reception of radiation with $\lambda = 1.06$ μm are presented in Fig.2. For $\lambda = 1.06$ μm the spectral sensitivity of realized device is two times more than the sensitivity of Si ones. It can see

photosensitivity spectrum semiwidth of InP-InGaAsP photoreceiver depends on InGaAsP ($E_g = 1.18$ eV) frontal layer thickness.

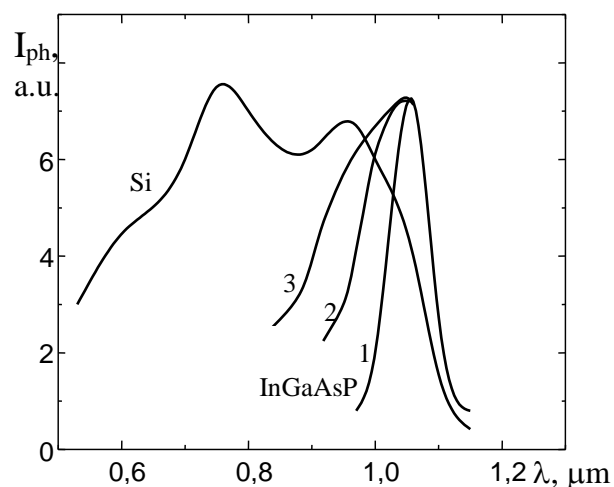


Figure 2. The spectral characteristics of selective InP-InGaAsP photodiode-quadrant and of Si photoreceiver.

Thickness of frontal layer InGaAsP ($E_g = 1.18$ eV): 1 – $d_2 = 7$ μm ; 2 – $d_2 = 4$ μm ; 3 – $d_2 = 2.5$ μm .

The spectrum semiwidth is 70 nm for layer thickness $d_1 = 7$ μm (Fig.2, curve 1). Red threshold of photosensitivity is moved to higher energy with decreasing frontal layer thickness (Fig.2, cur. 2,3). Photons with energy $h\nu < 1.12$ eV propagate whole structure without absorption, don't make any contribution to photocurrent forming. So, only photons with energy 1.12 eV $< h\nu < 1.18$ eV are absorbed in active layer, where space charge region of p-n junction is localized, form photocurrent of photoreceiver. Thus, the selective sensitivity is determined by frontal layer at short-wave side and by active layer at red boundary. Changing InGaAsP solid solution composition we can optimize structure for selective reception of radiation with different wavelength in spectral interval $0.96 < \lambda < 1.65$ μm and can diminish photosensitivity spectrum semiwidth to $20\div 30$ nm.

2. PHOTODIODES-QUADRANT FABRICATED ON THE BASIS OF SELECTIVE HETEROSTRUCTURES

2.1. The square photodiode-quadrant with four elements

The photodiode-quadrant of first variant (Fig.3) had a square photosensitive surface consisted of four photosensitive elements, which were separated by chemical etching and were

connected differential to ensure the two-coordinate sensitivity.

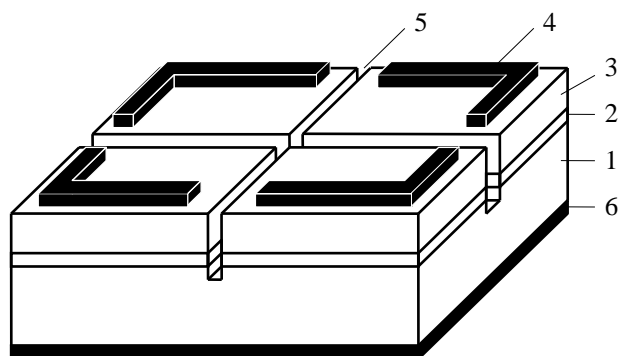


Figure 3. The square photodiode-quadrant with selective sensibility.

1 – n⁺InP substrate; 2 – InGaAsP ($E_g = 1.12$ eV) active layer; 3 – InGaAsP ($E_g = 1.18$ eV) frontal layer; 4 – frontal contact; 5 – channel formed by chemical etching; 6 – back contact.

The parameters of square photodiode-quadrant are presented in Table 1. The most imperfection of this photodiode-quadrant is the square shape, what didn't permit the effectively to utilize incident light flux having a circular spot form and so dependence between photocurrent and coordinate of light spot was nonlinear.

Table 1. Parameters of square photodiode-quadrant

Parameters	Values
Chip dimensions	$(2 \times 2) \cdot 10^{-2} \text{ cm}^2$
Photosensitive area	$1.7 \cdot 10^{-2} \text{ cm}^2$
Radiation wavelength in maximum photosensitivity	1.065-1.067 μm
Semiwidth of photosensitivity spectrum	85 - 110 nm
Absolute sensibility	0.51 - 0.57 A/W
Quantum efficiency	61 - 67 %
Open-circuit voltage	0.45 - 0.52 V
Saturation current	10^{-7} A
Dark current ($U = 1 \text{ V}$)	$10^{-5} - 10^{-6} \text{ A}$
P-n junction capacity ($U = 0$)	$(2-3) \cdot 10^3 \text{ pF}$
Series resistance	< 10 Ohm
Detectivity (calculated)	$1.7 \cdot 10^{11} \text{ cm} \cdot \text{W}^{-1} \cdot \text{s}^{-1/2}$
Abruptness of coordinate characteristic	$10^4 \text{ V} \cdot \text{W}^{-1} \cdot \text{mm}^{-1}$

2.2. The circular photodiode-quadrant with five elements

We elaborated and manufactured the selective photodiode-quadrant with new topology [4]. The second variant of photodiode-quadrant presented in Fig.4 has ensured the linear dependence between photoanswer and moving after "X" and "Y" coordinates. It has circular form and consists of five photosensitive elements: four of them are sectors of circle and are used for determination the position of incident light signal and the fifth is a protective peripheral ring, which signalizes the moment when incident signal begin to go out the device.

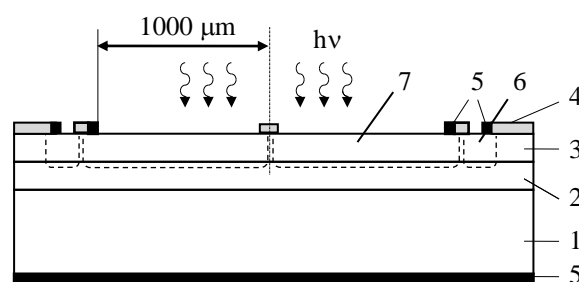


Figure 4. The circular photodiode-quadrant.

1 – n⁺InP substrate; 2 – InGaAsP ($E_g = 1.12$ eV) active layer; 3 – InGaAsP ($E_g = 1.18$ eV) frontal layer; 4 – SiO₂; 5 – contacts; 6 - protective peripheral ring; 7 – photosensitive quadrant sectors.

Electrical separation of the whole quadrant surface on the elements was made during the local Zn diffusion through the windows of SiO₂ mask. SiO₂ layer was deposited by chemical vacuum deposition. The contacts were formed by vacuum thermal evaporation of the metals (Au and Ni). Al₂O₃ layer used as an anti-reflecting covering was deposited by low temperature MOCVD method. The parameters of circular photodiode-quadrant are presented in Table 2.

Table 2. Parameters of circular photodiode-quadrant.

Parameters	Values
Whole area of device	$4.9 \cdot 10^{-2} \text{ cm}^2$
Photosensitive area of single quadrant sector	$6.7 \cdot 10^{-3} \text{ cm}^2$
Radiation wavelength in maximum photosensibility	1.06 μm
Semiwidth of photosensitivity spectrum	75 - 85 nm
Absolute sensitivity (for $\lambda = 1.06 \mu\text{m}$)	0.72 - 0.81 A/W
Quantum efficiency	76 - 84 %
Open-circuit voltage	0.53 - 0.57 V
Quadrant photosensitive sector capacity ($U = 0$)	200 pF
Dark resistance of quadrant photosensitive sector	$\leq 10 \text{ Ohm}$
Limit frequency for : $R_{\text{load}} = 8 \text{ kOhm}$ ($\tau = 4.5 \cdot 10^{-6} \text{ s}$) $R_{\text{load}} = 50 \text{ Ohm}$ ($\tau = 2 \cdot 10^{-8} \text{ s}$)	36 kHz 8000 kHz
Detectivity for interval $\Delta f = 300 - 10000 \text{ Hz}$	$2 \cdot 10^{11} - 3 \cdot 10^{12} \text{ cm} \cdot \text{Hz}^{1/2} \cdot \text{W}^{-1}$

For measuring the coordinate characteristics of photodiode-quadrant we used electric scheme of quadrant switching presented in Fig.5. The optic signal has a circular spot form with diameter equaled to radius of photodiode-quadrant sectors.

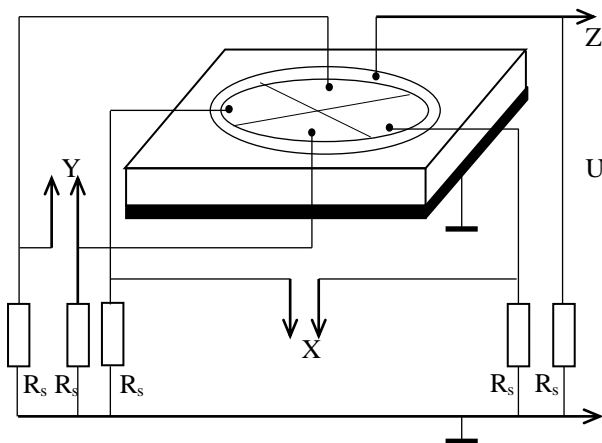


Figure 5. The electric scheme of quadrant switching for measuring the coordinate characteristics of photodiode-quadrant.

When the optic signal is symmetrical respecting the center photocurrents of those four circular sectors are equal. At optic signal moving after axes “X” or “Y” the difference between photocurrents of two opposite sectors linear increases depending on coordinate as are shown in Fig.6, curves X, Y. The peripheral ring signalizes the moment when optic signal begin to go out the photodiode-quadrant (Fig.6, curve Z).

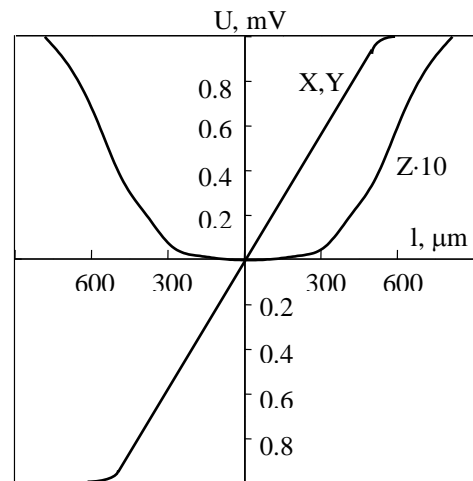


Figure 6. The coordinate characteristics of photodiode-quadrant.

The forward (a) and reverse (b) V-A characteristics of each photodiode-quadrant sector are shown in Fig.7. The dark current of each sector was determined by surface and bulk components. The ideality factor of the V-A characteristics for the first section was equal $2.0 \div 2.2$ and for second section was equal $1.3 \div 1.6$.

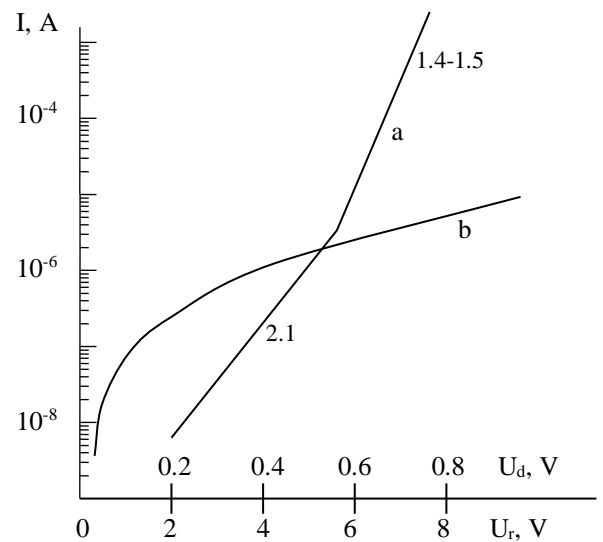


Figure 7. The typical dark V-A characteristics of photodiode-quadrant. a – forward, b – reverse characteristics.

The usual values of the dark current are $2 \div 400 \text{ nA}$ for bias voltage -0.5 V . The series resistance of the devices was less than 10 Ohm. It can see in Fig.8 the V-F characteristics of photodiode-quadrant were of $1/C^2 = f(U)$ type, that indicated p-n junction was abrupt.

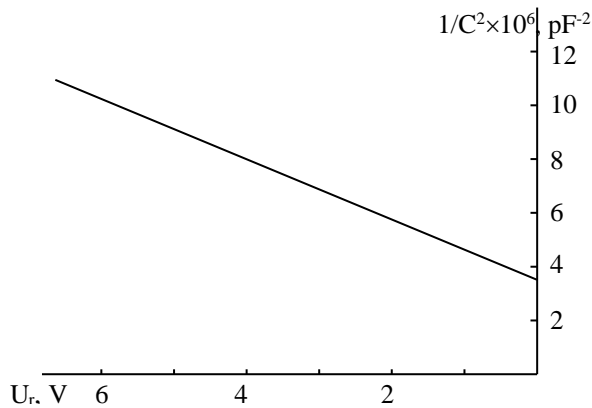


Figure 8. The V-F characteristic of photodiode-quadrant ($N_d \sim 2 \cdot 10^{16} \text{ cm}^{-3}$).

To determine the utilization fields of photodiode-quadrant were appreciated its limit possibilities. According to calculations and measurements, the photodiode-quadrant has an absolute spectral sensitivity $S = 0.6 \text{ A/W}$ for $\lambda = 1.06 \mu\text{m}$, an abrupt coordinate characteristic $K = 8 \cdot 10^3 \text{ V/(W}\cdot\text{mm)}$ and can be successfully used for receiving the unitary optic signals with impulse duration more than 10 ns and with incident optic power $\sim 1 \text{ mW}$ or for receiving the optic signals with limit frequency $\sim 20 \text{ MHz}$. The obtained values are extreme here because the relatively big area of photodiode-quadrant, necessary to ensure the coordinate characteristic, determines the big capacity of quadrant sectors. To extend the functional possibilities of photodiode-quadrant we have elaborated and manufactured a new structure with an integrated central detector [5].

2.3. The circular photodiode-quadrant with integrated central detector

The new structure ensures a selective spectral sensitivity with maximum for $\lambda = 1.06 \mu\text{m}$, an abrupt coordinate characteristic, the detection of unitary optic signals with impulse duration less than 10 ns or of optic signal with frequency more than 1 GHz. Fig.9 shows the structure section and the frontal view of selective photodiode-quadrant with integrated detector.

The structure of new device is much about the same as second variant. Photodiode-quadrant contains four elements having circular sector form and a protective peripheral ring. A circular photoelement with diameter $D_1 \leq 0.1 \cdot D_2$, where D_2 is diameter of photodiode-quadrant active surface, was made in the center of photodiode-quadrant.

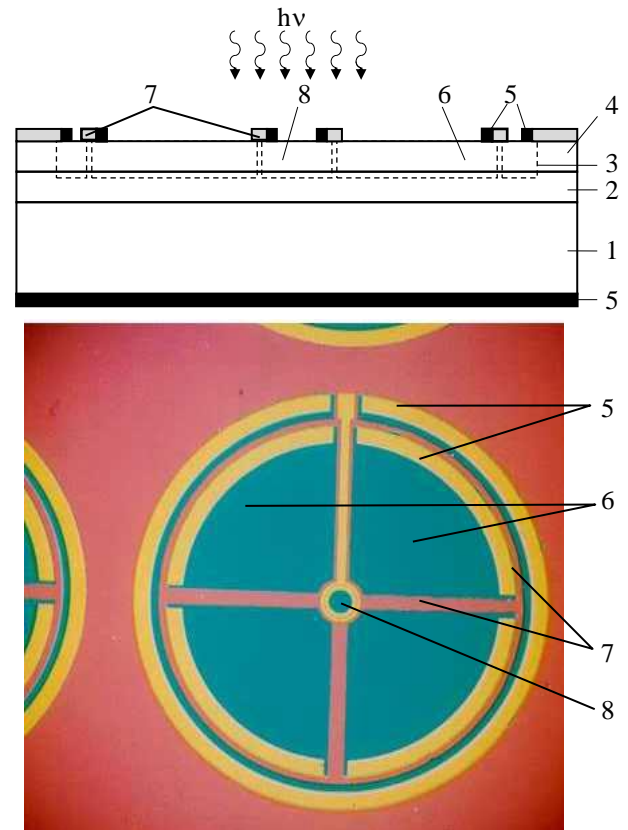


Figure 9. The structure and the frontal view of selective photodiode-quadrant with integrated detector.

1 – $n^+\text{InP}$ substrate, 2 – InGaAsP ($E_g = 1.12 \text{ eV}$) active layer, 3 – p-n junction, 4 - InGaAsP ($E_g = 1.18 \text{ eV}$) frontal layer, 5 – contacts, 6 - photosensitive quadrant sectors, 7 – SiO_2 , 8 – central detector.

Since coordinate characteristic is the most important we have estimated the influence of central detector upon it. Maximum voltage on the load resistance decreases less than 10 % for central detector diameter $D_1 = 400 \mu\text{m}$, but diameter 100 μm for detector active surface and 200 μm for whole central detector is quite enough. Since the central detector area is minimum 100 times less than photodiode-quadrant one, the presence of central detector didn't change the coordinate characteristic abruptness. On the other hand the central detector having a small area possesses a very low own capacity. It means that the time constant $\tau = R \cdot C$ gets small values, what permits to receive optic signals with frequency more than 1 GHz and unitary ones with impulse duration less than 10 ns. The parameters of photodiode-quadrant with central detector are presented in Table 3.

Table 3. The main parameters of photodiode

quadrant with integrated detector.

Parameters	Values
Chip dimensions	$3 \times 3 \text{ mm}^2$
Diameter of photodiode-quadrant	2.6 mm
Radius of photosensitive sectors	1 mm
Diameter of central photodetector	200 μm
Width of protective peripheral ring	150 μm
Width of metal contacts: of quadrant of central detector	100 μm 50 μm
Width of SiO ₂ separating strips	100; 50 μm
Radiation wavelength in maximum photosensitivity (λ_{max})	1.06 μm
Semiwidth of photosensitivity spectrum ($\Delta\lambda$)	75-85 nm
Absolute sensitivity (for $\lambda = 1.06 \mu\text{m}$)	0.72 - 0.81 A/W
Quantum efficiency	76 - 84 %
Own capacity of a quadrant photosensitive sector ($U = 0$)	190 pF
One sector capacity for reverse voltage $U_{\text{rev}} = 1.5 \text{ V}$	145 pF
Own capacity of central detector ($U=0$)	4 pF
Own capacity of central detector for reverse voltage $U_{\text{rev}} = 1.5 \text{ V}$	1.5 pF
Abruptness of coordinate characteristic	$8 \cdot 10^3$ $\text{V} \cdot \text{W}^{-1} \cdot \text{mm}^{-1}$
Work frequency	$> 1 \text{ GHz}$

For successfully using of photodiode-quadrant in optoelectronic systems of military and cosmic fields for space orientation of objects, a study of influence of cosmic radiation, particularly X-rays, upon the photodiode-quadrant main parameters is required [6,7]. For this purpose we made three series of photoreceivers with different thickness of both InGaAsP epitaxial layers: d_1 – thickness of active layer with $E_g = 1.12 \text{ eV}$, d_2 – thickness of frontal layer with $E_g = 1.18 \text{ eV}$. The p-n junction formed by local diffusion Zn is placed in different depths (h_{dif}) from surface. Main parameters of structures of these devices are:

Series 119

$d_1 = 2.5 \div 3 \mu\text{m}$; $n_1 = 5 \cdot 10^{16} \text{ cm}^{-3}$; $\mu_1 \approx 3000 \text{ cm}^2/(\text{V} \cdot \text{s})$
 $d_2 = 2.5 \div 3 \mu\text{m}$; $h_{\text{dif}} = 4.5 \mu\text{m}$

Series 167

$d_1 = 2.7 \div 3.3 \mu\text{m}$; $n_1 = 10^{15} \text{ cm}^{-3}$; $\mu_1 = 2500 \text{ cm}^2/(\text{V} \cdot \text{s})$;
 $d_2 = 4 \div 5.5 \mu\text{m}$; $n_2 = 10^{16} \text{ cm}^{-3}$; $\mu_2 = 2400 \text{ cm}^2/(\text{V} \cdot \text{s})$;
 $h_{\text{dif}} = 6 \mu\text{m}$

Series 169

$d_1 = 4 \div 6 \mu\text{m}$; $n_1 = 8 \cdot 10^{15} \text{ cm}^{-3}$; $\mu_1 = 1800 \text{ cm}^2/(\text{V} \cdot \text{s})$;
 $d_2 = 3.7 \div 4.5 \mu\text{m}$; $n_2 = 10^{16} \text{ cm}^{-3}$; $\mu_2 = 2000 \text{ cm}^2/(\text{V} \cdot \text{s})$
 $h_{\text{dif}} \approx 7 \mu\text{m}$

here n and μ are concentration and mobility of charge carries in active and frontal layers.

The structures were irradiated for a few times to achieve a summary dose of 760 kR. Dark currents of quadrant photosensitive sectors depending on X-ray summary dose for reverse voltage $U = -1.5 \text{ V}$ were measured, constructed and analyzed. They are shown in Fig.10.

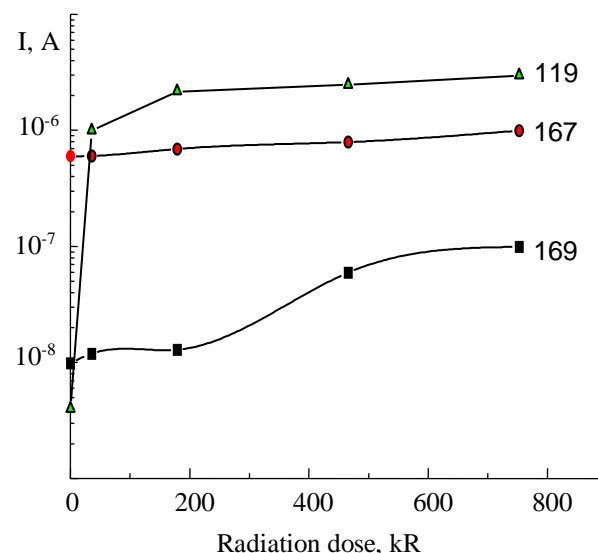


Figure 10. Dark currents depending on radiation dose.

One can see that photodiodes-quadrant with junction near frontal surface degrade more intensive. The second conclusion is: photodiodes-quadrant degrade intensive up to dose 100 kR.

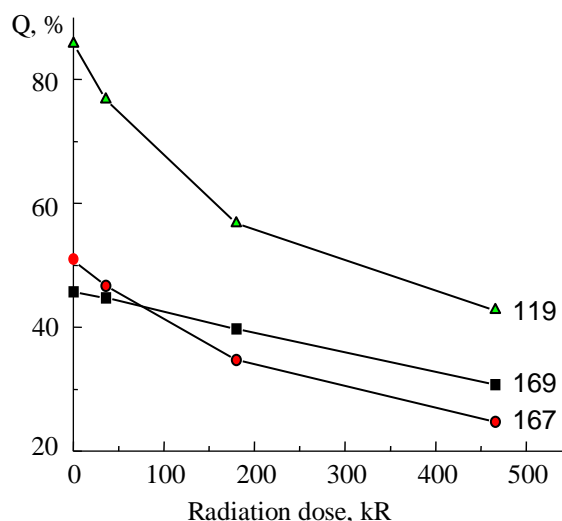


Figure 11. Quantum efficiency depending on radiation dose.

Degradation rate decreases abrupt with further dose increasing. This is demonstrated also by dependence “quantum efficiency – X-ray dose” (Fig.11). The summary dose of 466 kR reduces

external quantum efficiency with $\sim 40\%$ from its maximum value.

Photodiodes-quadrant with deeper p-n junction degrade less. Effected investigations show that the localization of p-n junction to a considerable depth from device surface is required to protect p-i-n photodiodes on the basis of InP-InGaAsP heterostructures from cosmic radiation, particularly from X-rays.

From this point of view photodiode-quadrant on the basis of InP-InGaAsP heterostructures are better than Si and Ge p-i-n photodiodes, because their frontal layer serving as optic filter can reduce considerable the influence of radiation upon the p-n junction, increasing the photoreceiver reliability.

3. CONCLUSIONS

Selective photoreceivers of optic signals transferred through atmosphere with high trouble protection were elaborated and manufactured on the basis of InP-InGaAsP heterostructures by liquid phase epitaxy and low temperature Zn diffusion. The spectral sensitivity of realized photoreceivers on the basis of InP-InGaAsP heterostructures is two times more for $\lambda = 1.06 \mu\text{m}$ than the sensitivity of Si ones. Changing composition of InGaAsP solid solution being frontal and active layers it is possible to optimize structure for selective reception of radiation with different wavelength in spectral interval $0.96 < \lambda < 1.65 \mu\text{m}$.

The elaborated and manufactured photoreceivers possess more large functional properties. High parameters of realized devices shown the efficiency of used technical decisions and possibility of successful using of these photoreceivers both as a photodiode-quadrant with coordinate sensitivity (coordinate characteristic abruptness $K = 8 \cdot 10^3 \text{ V} \cdot \text{W}^{-1} \cdot \text{mm}^{-1}$) and as a photodetector of high frequency ($f > 1 \text{ GHz}$) optic signals or of small duration ($t \leq 1 \text{ ns}$) unitary signals.

References

1. Dorogan V.V., Brynzari V.I., Korotchenkov G.S., Kosyak V.A. *Selective photodiode with two-coordinate sensitivity (quadrant) on the basis of InGaAsP quaternary compounds // Proc. of 20th Conf. on Microelectronics (MIEL'95), 1, pp.431-434, Nis, Serbia, 1995.*
2. Dorogan V., Brynzari V., Korotchenkov G., Snigur A., Kosyak V., Vieru T. *The photoreceivers*

on InGaAsP with advanced reliability and protection from optic background // Proc. of IVth Int. Conf. on Reliability of Semiconductor Devices and Systems (RSDS'96), pp.242-245, Chisinau, Moldova, 1996.

3. Dorogan V.V., Syrbu N.N., Cretsu R.V. *Formation of the InGaAs layers onto InP substrates by liquid-phase epitaxy // Optics Communications, 132, pp.449-451, 1996.*

4. Dorogan V., Brynzari V., Korotcenkov G., Coseac V., Vieru T., Necsoiu T., Savastru R. *Technology and designs are used for InGaAsP photodiodes fabrication // Optoelectronic, Romania, 4, no.2, pp.77-81, 1996.*

5. Dorogan V., Canțer V., Cacerea D., Brynzari V., Vieru T., Coseac V. *Selective photodiode-quadrant // Patent MD nr. 877 G2, AGEPI Rep. Moldova, 1997.*

6. Dorogan V., Samusi I., Rusanovschi M., Burbulea N., Vieru T., Coseac V. *Factors determining the quality and reliability of InP-InGaAsP epitaxial structures // Proc. of Int. Conf. on Microelectronics and Computer Science (ICMCS'97), 1, pp.25-28, Chisinau, Moldova, 1997.*

7. Dorogan V., Vieru T., Coseac V. *Influence of structural defects upon the InGaAsP p-i-n photodiode parameters // Proc. of 5th Symposium of Optoelectronics, pp.32-42, Bucharest, Romania, 1998.*